INTERFACE

royalsocietypublishing.org/journal/rsif

Research

Cite this article: Aiello BR, Sikandar UB, Minoguchi H, Bhinderwala B, Hamilton CA, Kawahara AY, Sponberg S. 2021 The evolution of two distinct strategies of moth flight. *J. R. Soc. Interface* **18**: 20210632.
https://doi.org/10.1098/rsif.2021.0632

Received: 4 August 2021
Accepted: 2 November 2021

Subject Category:
Life Sciences–Physics interface

Subject Areas:
biomechanics, biophysics, evolution

Keywords:
insect, wing, morphology, aerodynamics, moth, flapping flight

Author for correspondence:
Brett R. Aiello
e-mail: baiello3@gatech.edu

†These authors contributed equally to this study.

Electronic supplementary material is available online at https://doi.org/10.6084/m9.figshare.c.5713008.

THE ROYAL SOCIETY PUBLISHING

The evolution of two distinct strategies of moth flight

Brett R. Aiello[1,2,4,†], Usama Bin Sikandar[3,5,†], Hajime Minoguchi[1], Burhanuddin Bhinderwala[1], Chris A. Hamilton[6], Akito Y. Kawahara[4,7,8] and Simon Sponberg[1,2]

[1]School of Physics, [2]School of Biological Sciences, and [3]School of Electrical and Computer Engineering, Georgia Institute of Technology, Atlanta, GA 30332, USA
[4]McGuire Center for Lepidoptera and Biodiversity, Florida Museum of Natural History, University of Florida, Gainesville, FL 32611, USA
[5]Department of Electrical Engineering, Information Technology University, Lahore, Pakistan
[6]Department of Entomology, Plant Pathology and Nematology, University of Idaho, Moscow, ID 83844, USA
[7]Department of Biology, and [8]Department Entomology and Nematology, University of Florida, Gainesville, FL 32608, USA

BRA, 0000-0001-9034-0460; UBS, 0000-0003-3335-5994; HM, 0000-0002-4040-489X; CAH, 0000-0001-7263-0755; SS, 0000-0003-4942-4894

Across insects, wing shape and size have undergone dramatic divergence even in closely related sister groups. However, we do not know how morphology changes in tandem with kinematics to support body weight within available power and how the specific force production patterns are linked to differences in behaviour. Hawkmoths and wild silkmoths are diverse sister families with divergent wing morphology. Using three-dimensional kinematics and quasi-steady aerodynamic modelling, we compare the aerodynamics and the contributions of wing shape, size and kinematics in 10 moth species. We find that wing movement also diverges between the clades and underlies two distinct strategies for flight. Hawkmoths use wing kinematics, especially high frequencies, to enhance force and wing morphologies that reduce power. Silkmoths use wing morphology to enhance force, and slow, high-amplitude wingstrokes to reduce power. Both strategies converge on similar aerodynamic power and can support similar body weight ranges. However, inter-clade within-wingstroke force profiles are quite different and linked to the hovering flight of hawkmoths and the bobbing flight of silkmoths. These two moth groups fly more like other, distantly related insects than they do each other, demonstrating the diversity of flapping flight evolution and a rich bioinspired design space for robotic flappers.

1. Introduction

The evolution of flapping flight is foundational to the success of many insects [1] and is key for foraging, mate finding, courtship, predator avoidance and migration. To conduct these behaviours, significant selective pressures are placed on the flight performance of aerial organisms. Both wing morphology and movement can strongly impact the aerodynamics of a flying animal or machine [2,3]. For example, robotic flapping-wing micro air vehicles (FW-MAVs) have greater power efficiency and control than fixed-wing and rotary-wing aircraft of similar size [4,5]. Since the origin of flapping flight in insects, a wide diversity of wing morphologies (size, shape and mechanics), movements and flight behaviours have evolved [6–9]. A central question in the evolution of flapping flight is whether divergent strategies (combinations of wing shape, size and kinematics) arise to achieve similar flight performance. A comparison of disparate species across Insecta shows that not all insects use the same flapping flight strategies. Butterflies direct vortices in different directions on upstroke and downstroke [10,11], while a fly (*Drosophila melanogaster*) and a hawkmoth (*Manduca sexta*) produce lift on both upstroke and downstroke [3,12,13]. Mosquitoes use exceptionally high-frequency wingstrokes coupled

with rapid wing rotations [14] and dragonflies directly actuate the forewing and hindwing independently [15].

Less explored than these disparate comparisons is how closely related sister groups sharing morphological and physiological features diversify to fill different aeroecological niches. Do changes primarily occur in size, shape or kinematics to adapt single flight strategies to multiple behaviours or do all three change in tandem (different overall strategies) when new life histories and behaviours evolve? Considering diversification in closely related but divergent clades is an opportunity to test how wing size, shape and movement evolve together and interact to produce species-specific aerodynamics. However, these multiple factors contributing to aerodynamic performance make it challenging to link the evolutionary patterns of wing morphology and movement to interspecific differences in flight behaviour and aerodynamics as well as translate these patterns to the design and movement of engineered robotic flappers.

Hawkmoths (Sphingidae) and wild silk moths (Saturniidae) are diverse sister clades separated by approximately 60 Ma of evolution [9,16,17]. We recently showed that wing shape and size diverges between the families through an adaptive shift [9] coincident with the inter-familial divergence in life history [18–20] and flight behaviour [18–20]. However, wing morphology diverged between the clades in a way that belies simple intuition about how shape should affect performance based on the behavioural demands of each family [9]. Hawkmoths are active, fast fliers [20], well known for their ability to sustain long-duration bouts of hover [21–24], where some species can track flower oscillations up to frequencies of 14 Hz [24,25]. Yet, hawkmoths evolved small wings of high aspect ratio (AR), non-dimensional radius of the second moment of area ($\hat{r}_2$) and wing loading (W_s), metrics typically associated with power reduction and a high lift-to-drag ratio [9,26]. These metrics are also associated with poor manoeuvrability in fixed-wing aircraft, although animal fliers partially control flight more like rotary-blade systems where force vectors are modulated by wing rotations [27,28]. In contrast to the smoother flight of hawkmoths, silkmoth flight is often described as erratic or bobbing [18,29,30], which is thought to be advantageous for predator avoidance. Adult silkmoths also lack functional mouth parts and rely entirely on the strictly finite energy stores gathered during the larval period for their entire adult life stage [19]. Yet, silkmoths evolved wing morphology that is advantageous for manoeuvrability (low AR, W_s and $\hat{r}_2$), and, despite relying on a fixed energy budget as adults, the clade did not evolve wing morphology that is advantageous for power reduction [9]. It remains unclear if these shifts in wing morphology led to shifts in flight performance between the clades and how wing movement evolves in tandem and interacts with wing morphology to generate sufficient force to balance body weight while not exceeding the available power.

We hypothesize that each clade has evolved a distinct strategy for flight that relies on correspondingly distinct wing sizes, shapes and movements. If so, silkmoths and hawkmoths with comparable body masses should have similar wingstroke-averaged aerodynamic forces, but may differ in their within-wingstroke patterns of force production. Alternatively, the adaptive shift in wing morphology between the two clades [9] has a minimal impact on flight performance. A third alternative is that wing movement is conserved across the two clades and the divergence in wing morphology alone plays a role in flight performance, leading to the evolution of divergent flight performance between the two clades. While differences between Saturniidae and Sphingidae in wingbeat frequency and observations of erratic versus hovering flight suggest that kinematics play a role, morphology and movement have not been integrated in aerodynamic comparisons of the sister clades. To assess the interplay of shape, size and kinematics, we first quantify three-dimensional wing kinematics during forward flight from live specimens of five species from each sister family and combine these with our prior analysis of wing shape and size evolution [9]. We then use a blade element model [12,13,31] that can be applied across species to estimate the quasi-steady aerodynamic force production and power requirements and separate the contributions of wing size, shape and kinematics. As the notoriously agile hawkmoths evolved small wings of shapes advantageous for power reduction, we predict that the evolution of wing movement in this group aids in force production and flight control; both can be accomplished through high-frequency wingstrokes. We predict that the evolution of silkmoth wing movement reduces the power requirements of flight, which can occur through high-amplitude wingstrokes [32–34]. Alternatively, silkmoths have not evolved any means of reducing power, which could be an additional factor contributing to the short silkmoth adult lifespan. Revealing how species of each clade have evolved sufficient force generation within an available power budget through interspecific differences in wing shape, size and movement will also unveil multiple, and possibly unique, combinations of aerodynamic variables within a bio-inspired design space that could be implemented in future robotic fliers tuned to various behavioural and performance metrics.

2. Material and methods

Details of the mathematical notation used in this study are in electronic supplementary material, table S1.

2.1. Live specimens

Live specimens of five different species from each sister family (10 total species) were used in this study (electronic supplementary material, table S2). Species from the hawkmoth (Sphingidae) family include: *Eumorpha achemon*, *Amphion floridensis*, *Hyles lineata*, *Paonias myops* and *Smerinthus ophthalmica*. Species from the silkmoth (Saturniidae) family include: *Actias luna*, *Automeris io*, *Antheraea polyphemus*, *Hyalophora euryalus* and *Eacles imperialis*.

2.2. Body and wing measurements and morphometrics

Body and wing morphologies were digitized for each live specimen using StereoMorph (v. 1.6.2) [35] in R (v. 3.4.2) following our previous methodology [9]. For all individuals, total body mass (m_t) was measured directly after the individual was flown.

Morphology was analysed in Matlab (v. R2018b - 9.5.0.944444) following [9]. To generate a combined wing shape from the overlap of the fore- and hindwings, the forewing long axis was rotated to be perpendicular to the body long axis. In hawkmoths, the long axis of the hindwing was also oriented perpendicular to the body long axis. In silkmoths, hindwing orientation was left in its natural position obtained when the wings are splayed open and the moth is at rest. This position was chosen while reviewing videos of silkmoth flight; the long axis of the hindwing is always oriented posteriorly and nearly parallel with the body long axis (see electronic supplementary material, movies). All wing morphology parameters (see

electronic supplementary material) for aerodynamic analysis were calculated from the combined wing following [36].

2.3. High-speed recordings of moth flight

Flight experiments were conducted in a 100 × 60.96 cm working section of an open-circuit Eiffel-type wind tunnel (ELD, Inc., Lake City, MN, USA). See [37] for tunnel details.

Moths were enticed to fly by providing a wind speed of 0.7 ms^{-1}. Flight bouts were filmed at 2000 frames s^{-1} for hawkmoths and 1000 frames s^{-1} for silkmoths using three synchronized high-speed cameras (resolution: 1280 × 1024 pixels) (Mini UX 100; Photron, San Diego, CA, USA). The wind tunnel was illuminated with six 850 Nm infrared lights (Larson Electronics, Kemp, TX, USA) and a neutral density-filtered white LED 'moon' light (Neewer CW-126) [24]. Room lights were also turned on for the diurnal species (*A. floridensis*).

Videos were digitized and calibrated in XMALab [38]. A total of seven landmarks were digitized on the moth: rostral tip of the head (between the antennae), junction between the thorax and abdomen, caudal tip of the abdomen, left and right forewing hinges, right wing tip and a point on the trailing edge of the wing (see electronic supplementary material, table S3 for individual kinematics).

2.4. Blade element model summary

A third-order Fourier series was fitted to all kinematics for every wingstroke. Representative wing shape, size and kinematics for each species were calculated by averaging the wing shapes and time-varying Fourier-fitted kinematics over all wingstrokes of all individual moths.

Species-specific aerodynamic forces were evaluated using a quasi-steady blade element model, estimating the total aerodynamic force as contributions from translational and rotational motion and the force due to added mass [12,13,31,39] and based on hawkmoth (*Manduca sexta*) lift and drag coefficients [13]. This type of first-principles model provides flexibility to directly test how different combinations of wing morphology and kinematics impact aerodynamic force and power across a larger number of species and allows us to directly explore how the different force components (translational, rotational and added-mass) contribute to the overall aerodynamic force profile. A trim search then found equilibrium conditions to balance force and moment over a wingstroke. Trim conditions are given in electronic supplementary material, table S4.

The wing inertial force was also calculated. Since these are internal forces to the moth, they cannot produce a net force over full steady wingstroke periods, but it is possible that there is an indirect contribution of wing inertial forces on aerodynamics via their movement of the body. However, the wing kinematic measurements were relative to the body and we transformed all forces to the body-attached frame. Thus, any relative motion between the wings and body due to inertial forces and its effect on the aerodynamics is naturally captured.

Total aerodynamic power is the sum of induced, profile and parasite powers [33], and we also calculate the inertial power. A detailed formulation of the blade element model is in the electronic supplementary material.

3. Results

3.1. Hawkmoths and silkmoths evolved divergent wing and body morphology

We quantified several morphological features and compared them with our previous work to ensure that the previously identified inter-clade differences in wing and body morphometrics are consistent. Variables include wing area (S), the non-dimensional radius of the second moment of wing area ($\hat{r}_2$), wing aspect ratio (AR), wing loading (W_s) and total body mass (m_t) (summary data: electronic supplementary material, table S2).

Hawkmoth and silkmoth wing morphology is well separated in morphospace (figure 1*a–c*). A MANOVA where AR, W_s and $\hat{r}_2$ are the response variables and clade is the factor reveals significant differences between clades ($F = 34.5$, $p < 0.0001$). AR, W_s and $\hat{r}_2$ are all greater in hawkmoths than in silkmoths by factors of 1.6, 3.7 and 1.1, respectively. Variation in body mass (m_t) spans similar ranges within each family. For a given body mass, S is significantly greater in silkmoths than in hawkmoths (figure 1*d*), as indicated by an ANCOVA between the slopes of each clade (hawkmoth regression: $r^2 = 0.9565$, $F = 263.7$, $p < 0.0001$; silkmoth regression: $r^2 = 0.6273$, $F = 15.15$, $p = 0.0036$; ANCOVA: $F = 26.551$, $p < 0.0001$). These results recapitulate the broader adaptive shift that we found in wing and body morphology in prior work.

3.2. Hawkmoths and silkmoths evolved divergent wing kinematics

Wing movement can also strongly impact aerodynamics. We next determined if wing movement diverged between the clades. Analysis of three-dimensional kinematics across all 10 species revealed strong and consistent inter-clade differences for several variables (figure 2; electronic supplementary material, table S3; recorded kinematics: hawkmoths, electronic supplementary material, figure S4; silkmoths, electronic supplementary material, figure S5). Across the species considered here, hawkmoths fly with a 2.5 times greater average wing beat frequency (n) than silkmoths. Silkmoths fly with a 1.2 times greater average sweep amplitude (ϕ_{p-p}) and 2.3 times greater average inclined (more vertical) stroke plane angle (β) than hawkmoths (electronic supplementary material, table S3). A MANOVA where n, $\overline{\phi}$ and β are the response variables and clade is the factor reveals significant differences between clades ($F = 32.546$, $p < 0.0001$).

The within-wingstroke time-varying deviation angle (θ) and feathering angle (α) differed slightly between hawkmoths and silkmoths (figure 2*a*,*b*; electronic supplementary material, figures S4 and S5). On average, silkmoths had 1.5 times larger θ amplitude, whereas hawkmoths had 1.2 times larger α amplitude and 1.1 times smaller mean α. These differences are also evident when comparing an exemplar from each clade: *E. achemon* (hawkmoth) and *A. polyphemus* (silkmoth) (figure 2*a*).

3.3. Hawkmoths and silkmoths evolved convergent wingstroke-averaged aerodynamics and aerodynamic power requirements

Given that hawkmoths and silkmoths evolved differences in wing shape, size and movement, we assessed the overall aerodynamic force and power implications between the two clades. Again, while we focus on two exemplar species (figure 3*a*)—the hawkmoth, *E. achemon*, and the silkmoth, *A. polyphemus*—these trends are consistent across the species of each respective family (electronic supplementary material, figure S6). Despite the large morphological differences, hawkmoths and silkmoths have overlapping total body masses, suggesting that they produce comparable

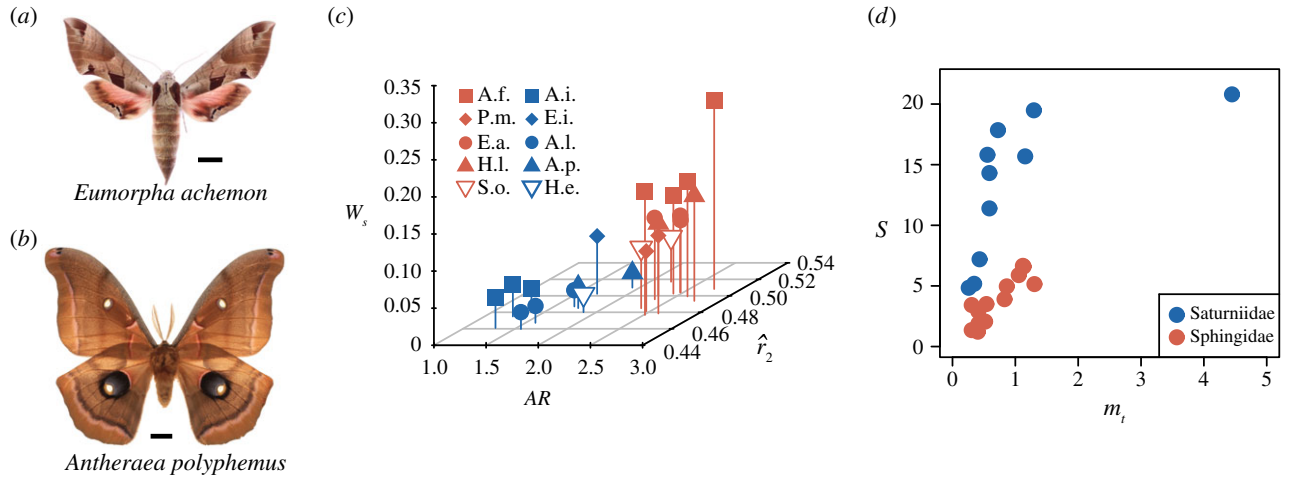

Figure 1. Wing shape and size is divergent between hawkmoth and silkmoth species. (*a*) A representative hawkmoth (*E. achemon*) and (*b*) silkmoth (*A. polyphemus*) species used for a detailed comparison of wing kinematics and aerodynamics. Scale bar length = 1 cm. (*c*) Functionally relevant metrics of wing morphology and (*d*) wing size diverge between hawkmoths and silkmoths.

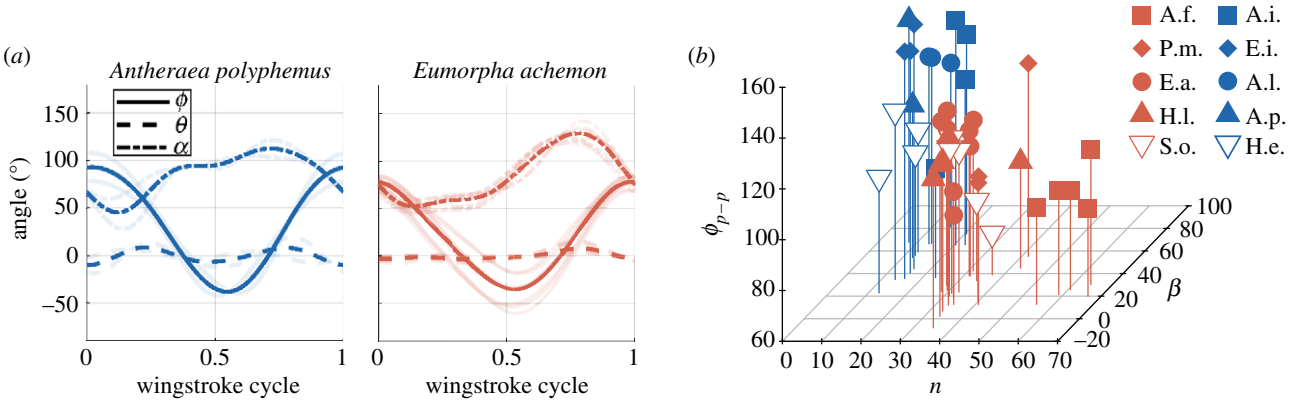

Figure 2. Wing kinematics are divergent between hawkmoths and silkmoths. (*a*) Within-wingstroke kinematics of the sweep (ϕ), deviation (θ) and feathering angles (α) for each of the representative species: *E. achemon* (hawkmoth) and *A. polyphemus* (silkmoth). (*b*) Summary kinematics of wingstroke amplitude (ϕ_{p-p}), frequency (n) and stroke plane angle (β) for all 10 species used in this study. The key for species abbreviations for each symbol can be found in electronic supplementary material, table S1.

aerodynamic forces at steady state. We found that all species were able to trim to equilibrium conditions using the observed wingstroke kinematic variation in each species and prior observed variation in C_L and C_D (electronic supplementary material, table S4). *Actias luna* was an exception in that its forces trimmed, but a small pitching moment persisted in the model. Thus, the combinations of wing shape, size and kinematics, despite being significantly divergent, produce comparable wingstroke-averaged aerodynamic forces (electronic supplementary material, figure S6). In addition, the peak magnitudes of the wing inertial forces are of the same order of magnitude as the aerodynamic forces across all species (electronic supplementary material, figure S10).

Similar average aerodynamic forces do not imply similar aerodynamic power across clades. Nonetheless, the power requirements of forward flight are also consistent within and between each clade. Total body mass-specific aerodynamic power requirements range from 15.06 to 18.32 W kg^{-1} in hawkmoths and from 11.76 to 17.18 W kg^{-1} in silkmoths (figure 4*a*). However, there were differences in which component of aerodynamic power contributed greatest. Induced power (P_{ind}) was always the largest contributor to total power in hawkmoths and three silkmoths species, but in two silkmoths (*A. luna* and *A. polyphemus*) profile power (P_{pro}) was greater than P_{ind} (figure 4*a*). Parasitic power (P_{par}) was negligible across all species (figure 4*a*), consistent with prior studies [33].

3.4. Hawkmoths and silkmoths evolved divergent wingstroke-averaged inertial power requirements

While aerodynamic power requirements are similar between the species of each family, the inertial power requirements, the power required to accelerate and decelerate the wing mass, do differ between the families (electronic supplementary material, table S5). On average, the inertial power (body-mass specific) of hawkmoths (36.7 ± 12.8 Wkg^{-1}) is approximately three times greater than that of silkmoths (13.4 ± 3.3 Wkg^{-1}). The difference is primarily driven by the large inter-clade difference in n as inertial power scales with n^3. However, these inter-clade differences in inertial power probably do not contribute to larger inter-clade differences in power consumption. Most of the energy required to accelerate and decelerate the wing mass is believed to be

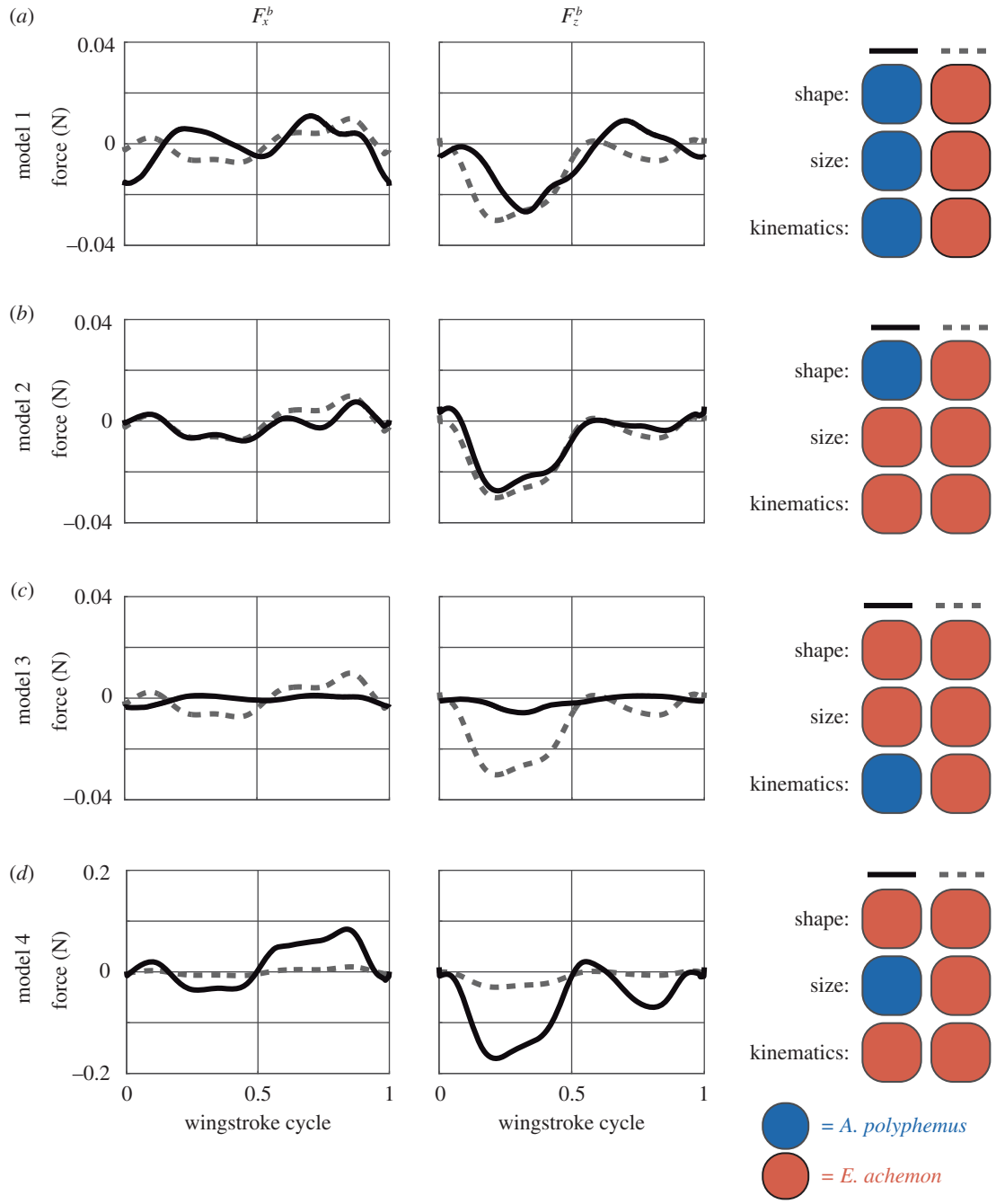

Figure 3. Quasi-steady aerodynamic force production by the right wing in a body-centred coordinate frame where the positive *z*-axis points in the direction of gravity. The two wings of each model are identified by solid and dashed lines, respectively. The dashed line is the same in each model. The colours on the right side indicate the specific morphology and movement parameters used for each model. Blue represents variables from *A. polyphemus* and red represents variables from *E. achemon*. (*a*) model 1 compares interspecific aerodynamics between *A. polyphemus* (solid line) and *E. achemon* (dashed line). Models 2 (*b*), 3 (*c*) and 4 (*d*) investigate aerodynamic impact by changes in wing shape, movement and size, respectively. All forces are only presented for a single right wing. The negative F_z^b direction points upwards and the positive F_x^b direction points forwards. Note that the scale of the *y*-axis changes in model 4 (*d*). The large force magnitudes of the solid line model of model 4 (*d*) result from this model using the larger wing size of *A. polyphemus* and the faster wing beat frequency of *E. achemon*, both of which strongly impact the magnitude of force production.

stored and returned through thoracic mechanics [40,41]. Even if the inertial power requirement is not fully accounted for by elastic energy exchange, it is not surprising that the remaining power requirement is greater in hawkmoths than in silkmoths since most hawkmoth species regularly feed and replenish energy stores. Comparative work is lacking on thoracic mechanics and elastic energy storage, but, given that silkmoths lack functional mouthparts as adults, we hypothesize that thoracic mechanics might have also evolved to increase the ability to store and return elastic energy and thus reduce the energy expenditure needed to move the wing masses. We find this a particularly exciting avenue of future research.

3.5. Hawkmoths and silkmoths evolved interspecific differences in within-wingstroke aerodynamics

While the average powers and normalized forces converge, the within-wingstroke force profiles do show consistent differences between clades, reflecting different strategies for achieving body weight support and thrust. In hawkmoths, F_x^b is predominately negative (backwards) during the first

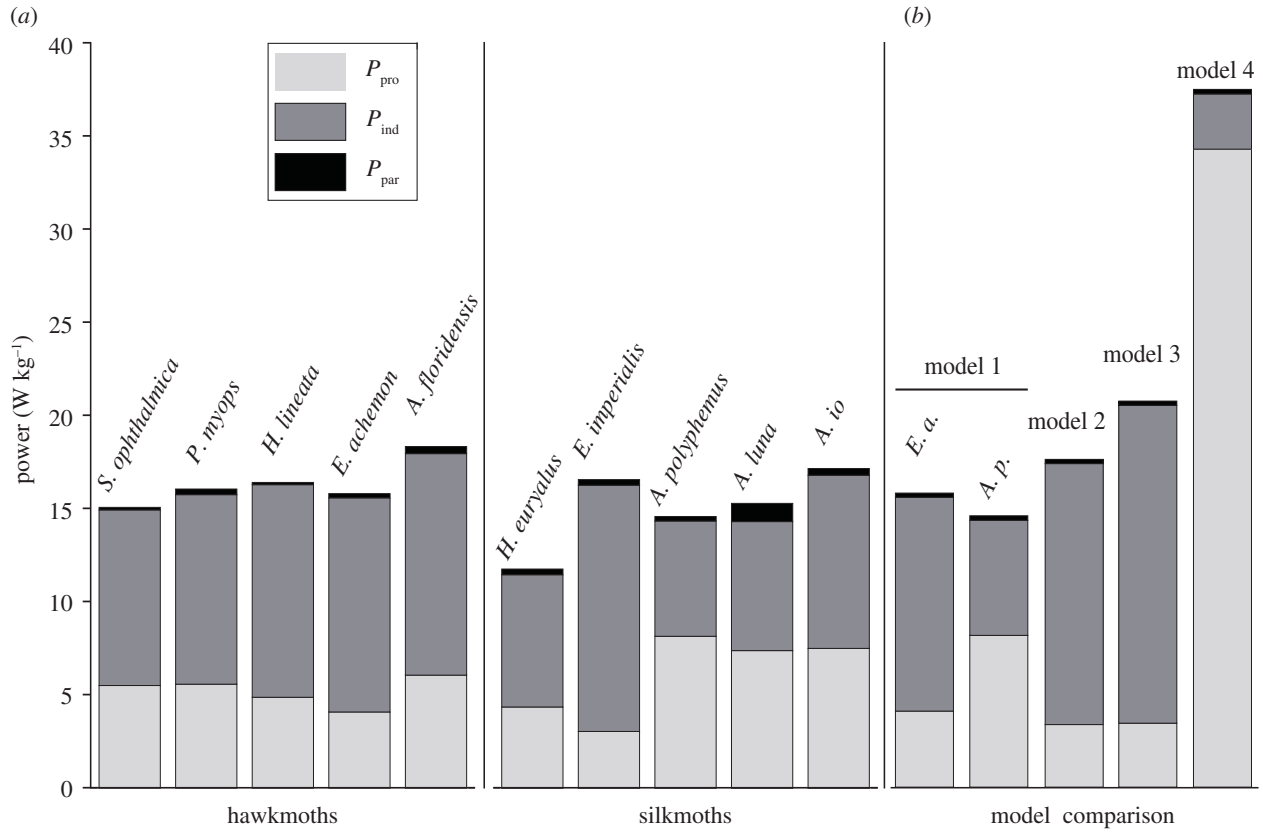

Figure 4. A comparison of the total aerodynamic power requirements of flight. Total aerodynamic power is the sum of induced power (P_{ind}), profile power (P_{pro}) and parasitic power (P_{par}). The total and component power is shown for (*a*) all species during forward flight at recorded speeds and (*b*) each sub-model of our two-species comparison in figure 3*b–d*.

half and positive during the second half of the wingstroke. In silkmoths, F_x^b has significant positive and negative portions during both halves of the wingstroke (figure 3*a*; electronic supplementary material, figure S6). In hawkmoths, F_z^b generally supports weight (negative) across the entire wingstroke and is of greater (more than twice) magnitude during the first half than during the second half wingstroke (figure 3*a*; electronic supplementary material, figure S6). In silkmoths, F_z^b is also generally negative, but is usually of reduced magnitude during the second half stroke in comparison with hawkmoths; in two silkmoth species, F_z^b becomes predominantly positive (figure 3*a*; electronic supplementary material, figure S6). Although the magnitudes of rotational (F_{rot}^b) and added mass (F_{adm}^b) forces are generally larger in silkmoths than in hawkmoths (electronic supplementary material, figures S6 and S7), these forces tend to act in opposition, and, across all species, interspecific differences in total force (F_{total}^b) are primarily due to translational force, F_{tra}^b (electronic supplementary material, figures S6 and S7). The silkmoth *A. io* represents an exception to this as F_{total}^b is indeed impacted by F_{rot}^b and F_{adm}^b throughout the wingstroke (electronic supplementary material, figure S6). These results are consistent whether we consider the species-specific flight speeds or model all species at 2 m s^{-1} (electronic supplementary material, figure S8).

3.6. Quasi-steady blade element models separate the contributions of wing shape, size and kinematics in flight strategies

We created several intermediate models to separate contributions and assess how size, shape and kinematics impact aerodynamics. To do so, we focused on exemplar species from each clade (*E. achemon*, *A. polyphemus*), which are representative of the general divergence in wing shape, size and movement between the clades. The base comparison reported above (model 1—figure 3*a*; electronic supplementary material, figure S7A-B) uses each species' own wing shape and size, time-varying kinematics (ϕ, θ, α, β, χ and n) and recorded forward flight velocities. In model 2 (figure 3*b*; electronic supplementary material, figure S7C) kinematics and size are set to those of the hawkmoth *E. achemon* in both cases, leaving interspecific differences only in wing shape. In model 3 (figure 3*c*; electronic supplementary material, figure S7D), wing shape and size are set to those of *E. achemon*, leaving interspecific differences only in wing kinematics. Finally, in model 4 (figure 3*d*; electronic supplementary material, figure S7E), wing shape and kinematics are set to those of *E. achemon*, leaving interspecific differences only in wing size.

3.6.1. Wing shape

The *E. achemon* wing shape produces slightly larger net aerodynamic force than *A. polyphemus* shaped wings (model 2, figure 3*b*; electronic supplementary material, figure S7C). The increase in F_{total}^b is primarily driven by the increased F_{tra}^b (electronic supplementary material, figure S7C). While different in average and peak magnitude, the pattern of the F_{tra}^b (as well as F_{rot}^b and F_{adm}^b) throughout the wingstroke was similar in both wing shapes (electronic supplementary material, figure S7C). The *E. achemon* wing shape produced larger F_{tra}^b because of its larger radius of second moment of area than *A. polyphemus*.

3.6.2. Wing kinematics

The most apparent aerodynamic interspecific difference due to kinematics alone (model 3) is that *A. polyphemus* kinematics produces a lower force (five times smaller peak force) than *E. achemon* kinematics (figure 3*c*; electronic supplementary material, figure S7D). The reduction in F^b_{total} is again determined primarily by differences in F^b_{tra} (electronic supplementary material, figure S7D). The main cause of this difference is that n, and hence wing angular velocity, of *E. achemon* is approximately three times greater than that of *A. polyphemus* (figure 2; electronic supplementary material, table S3). Interspecific differences in kinematics are also responsible for interspecific differences in the sign of F^b_x and F^b_z in model 1 during the first half and second half of wingstroke, respectively (figure 3*a*). To break this down further, we separated the contributions of stroke plane angle (β), wing angles (ϕ, θ and α) and n (electronic supplementary material, figure S9). The interspecific sign flip in F^b_z (figure 3*a*) occurs as a result of n (electronic supplementary material, figure S9B), and the F^b_x sign flip (figure 3*a*) occurs primarily from differences in lower n and more vertical β of *A. polyphemus* (electronic supplementary material, figure S9B,C).

3.6.3. Wing size

A. polyphemus has 2.5 times larger wings and, if all other variables are equal (model 4), it is not surprising that *A. polyphemus* wing size produces about six times larger forces (figure 3*d*; electronic supplementary material, figure S7E). As before, differences in F^b_{total} are primarily due to differences in F^b_{tra} (electronic supplementary material, figure S7E). However, the F^b_{rot} and F^b_{adm} components of F^b_x and F^b_z are also nearly an order of magnitude larger in *A. polyphemus* sized wings than in *E. achemon* sized wings (electronic supplementary material, figure S7E). Overall, wing size has the predictable effect of scaling force components.

4. Discussion

4.1. The evolution of two distinct strategies for flapping flight

Silkmoths and hawkmoths have evolved two distinct strategies (combinations of wing shape, size and movement) for flapping flight (figure 5). Species of both families have evolved sufficient average force production and power reduction, but do so with distinctly different wing shapes, sizes and movements and different patterns of within-wingstroke force production. An adaptive shift in hawkmoth wing size and shape resulted in the divergence of wing morphology between the two clades [9]. In the present study, we now demonstrate that key wing movement features also diverge between clades, indicating that hawkmoth wing movements, which occur at frequencies more than three times greater than silkmoths (figure 2), might also be evolving around an adaptive peak.

In hawkmoths, sufficient force production is primarily due to the evolution of high n (movement) (figure 2) because translational force production, the largest contributor to total force, is proportional to airflow velocity squared [32]. The evolution of higher $\hat{r}_2$ wings (shifting more area distally) in hawkmoths also enhances the force and torque production (e.g. [42,43]) compared with silkmoths. Silkmoths achieve sufficient force production through relatively larger wings than hawkmoths (figure 1*d*) because wing area is proportional to translational force and larger wings will also produce greater wing tip velocities [32]. So, hawkmoths primarily use kinematics to enhance the force production, whereas silkmoths primarily use wing shape and size.

Both clades are also likely under selective pressure to reduce the power requirements of flight. Hawkmoths regularly sustain long-duration bouts of hovering, often associated with nectaring from flowers [21,23–25], which requires a high power output [33], while all silkmoths do not feed as adults, relying on limited energy reserves gathered as larvae [18,19]. Hawkmoths evolved high AR wings (shape) ([9]; figure 1*c*), reducing the induced power (P_{ind}) requirements of flight [44,45] in comparison with the evolution of low AR in silkmoths (figure 4*b*). Silkmoths evolved high-amplitude wingstrokes (ϕ_{p-p}), also reducing P_{ind} (figure 4*b*), which is inversely proportional to both wing size (R) and ϕ_{p-p} [32,34]. In total, silkmoths have a lower P_{ind} than hawkmoths (figure 4*a*), offsetting the larger profile power (P_{pro}) incurred by the evolution of larger wings in silkmoths than hawkmoths, which ultimately results in similar overall power requirements between the clades (figure 4*a*). Thus, the evolution of hawkmoth wing shape and silkmoth wing movement are different means to reduce power.

Aerodynamic performance, therefore, emerges from the interaction of wing shape, size and kinematics, demonstrating an example of correlated evolution between the components of a complex locomotor system [46]. The ability for natural selection to act on both wing shape and kinematics to impact force generation and the power requirements of an animal demonstrates the potential decoupling of animal locomotor performance metrics. Because wing shape, size and movement can each independently affect aerodynamic performance, there are likely to be fewer purely morphological constraints forcing convergence. This may contribute to the diversity of wing shapes across extant aerial animals, even in closely related sister clades.

4.2. The evolution of two distinct aerodynamic strategies contributes to inter-clade differences in flight behaviour

4.2.1. Large, slow wings contribute to bobbing flight behaviour in silkmoths

While the two strategies contribute comparable average aerodynamic forces and power, inter-clade differences in within-wingstroke aerodynamics (figure 3*a*) probably contribute to differences in flight behaviour between the clades. Silkmoths often display erratic flight patterns [18,19,29,30] where vertical position is regularly changing throughout their flight bout. While all species produce sufficient F^b_z for forward flight, silkmoths generally have more variation in F^b_z between the first and second half of the wingstroke than hawkmoths (figure 3*a*; electronic supplementary material, figure S6). This is especially noticeable in *A. polyphemus* and *A. luna*, where F^b_z switches sign to become positive during the second half of the wingstroke. Large, slow force fluctuations and asymmetry (figure 3*a*; electronic supplementary material, figure S6) do lead to greater fluctuations in body vertical velocity (electronic supplementary material, figures S4 and S5; table S3) and are likely to be the source of the bobbing. Such erratic motions in silkmoths might be useful in

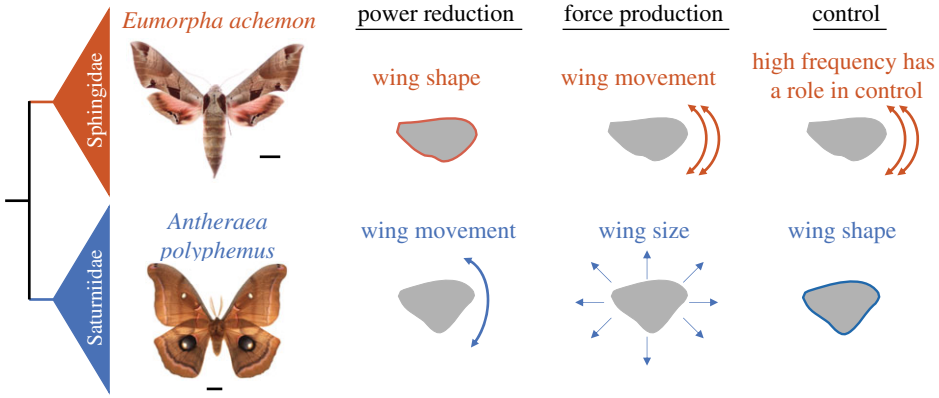

Figure 5. The evolution of two distinct strategies for flight. A summary of how distinct divergence in wing shape, size and movement impacts flight performance in each clade.

predator avoidance and may limit power minimization despite fixed energy budgets as adults.

The generation of wing inertial forces might also contribute to within-wingstroke bobbing and pitching of silkmoths. While inertial forces generated by the wings do not contribute to the overall trajectory of the centre of mass of the moth body, these forces can cause changes to the instantaneous trajectory of the body in the global frame, and thus contribute to within-wingstroke body movements such as pitching and bobbing. Although hawkmoths produce greater peak inertial forces than silkmoths, the significantly higher wing beat frequency of hawkmoths limits their ability to manifest large body oscillations over the course of the wingstroke in comparison with the lower wingbeat frequency (and thus greater wing beat cycle duration) of silkmoths. Thus, in addition to the contribution from aerodynamic force (figure 3*a*; electronic supplementary material, figure S6), inertial force can also contribute to the pitching and bobbing motion of the body, particularly in silkmoths owing to their lower wingbeat frequencies.

4.2.2. Evolution of high wing beat frequency (*n*) could contribute to hawkmoth manoeuvrability

The divergence of *n* parallels the divergence of flight behaviour [18–20] and wing morphology [9] between hawkmoths and silkmoths. The evolution of high *n* might be the key to conducting high-speed manoeuvres in small flapping fliers with high AR wings like hawkmoths. While we do not directly measure manoeuvrability in this study, it is clear that hawkmoths have evolved a means to accomplish rapid manoeuvres while foraging [21,24,25]. Since moths use flapping wing mechanics, it may not be surprising that they diverge from manoeuvrability metrics often associated with fixed-wing systems. As opposed to fixed-wing cases, manoeuvrability of flapping flight relies on the generation of aerodynamic forces from wing movement to initiate directional change [47]. Therefore, an increase in *n* would allow for more frequent modification of force vectors, which could increase manoeuvrability. Further, increasing *n* will also enhance manoeuvrability by increasing the force and torque produced by a wing [48], which is exemplified in model 3 of this study (figure 3*c*). The diversification of *n*, which supports our previous estimates based on scaling relationships [9], could contribute to interspecific variation in flight control and manoeuvrability across species. Therefore, we suggest that high *n* is one of the aspects of flight control that evolved in hawkmoths allowing for the completion of high-frequency manoeuvres.

4.3. Hawkmoth and silkmoth aerodynamics are more similar to other flying insects than they are to each other

Despite being sister clades, the respective flight strategies of hawkmoths and silkmoths are more similar to other flying insects than they are to each other. The hawkmoth flight strategy is most similar to that of other high-frequency flappers such as flies. In both hawkmoths (figure 3*a*; electronic supplementary material, figure S6) and the fly *D. melanogaster*, vertical force is produced during both halves of the wingstroke [49,50]. The low-frequency flapping and time-varying aerodynamics of silkmoths are most similar to those of butterflies. Across multiple species of butterflies and silkmoths, vertical force produced during the downstrokes acts to offset body weight while vertical force during the upstroke contributes either minimal or negative body weight support (figure 3*a*) [10]. As silkmoths and butterflies converged in wing shape [8], relative size [8], kinematics [10] and aerodynamics [10], it is not surprising that many species of both groups also evolved erratic flight. Similarly, species of both clades also evolved similar aerodynamic power requirements [10]. As butterflies feed as adults and silkmoths do not, the convergent power requirements suggest that silkmoths have not evolved any adaptations for additional power reduction in comparison with butterflies. The combination of wing morphology and kinematics that have evolved in both silkmoths and butterflies might be constrained for this style of flight. Finally, bumblebee aerodynamics at slow flight speeds are similar to that of hawkmoths, but, at fast flight speeds, vertical force production is asymmetric between first and second wingstroke halves [51], similar to a silkmoth (figure 3*a*). The shift in bee aerodynamics is due to an increasingly more vertical stroke plane at greater flight speeds (similar to silkmoths) [52], further exemplifying how the evolution of divergent kinematics between hawkmoths and silkmoths contributes to inter-clade differences in aerodynamics and flight behaviour.

In conclusion, the divergence in flight strategy between the hawkmoth and silkmoth sister clades is just as strong as the evolutionary divergence between distant clades. Through a strong divergence in wing shape, size and movement,

hawkmoths and silkmoths have evolved two independent flight strategies. This study thus demonstrates that even closely related clades with recently shared ancestry can still undergo strong divergence in flight strategies. The change in wing size and shape corresponds to an adaptive shift between silkmoths and hawkmoths [9], which is now reflected in their kinematics and performance. These sister groups are ideal 'model clades' [53] for exploring the morphological, neuromechanical and behavioural diversification of insect flight. Finally, while the design of human-engineered flapping fliers is often inspired by insect flight, a rich design space might be better inspired by the many strategies that even closely related insects take to achieve similar but flexible flight behaviours. Rapid manoeuvres through a cluttered environment and long sustained bouts of flight are two examples of such behaviours that can be incorporated into an FW-MAV. Indeed, this work illuminates a rich morphological and kinematic bio-inspired design space where different combinations of wing size, shape and movement can be implemented in FW-MAV design to improve flight performance fine-tuned to specific application.

Data accessibility. Data are available from the Dryad Digital Repository: https://doi.org/10.5061/dryad.3ffbg79jp [54].

Authors' contributions. Conceptualization: B.R.A. and S.S.; data curation: B.R.A., U.B.S., H.M., B.B., C.A.H., A.K.Y. and S.S.; formal analysis: B.R.A., U.B.S., H.M. and B.B.; funding acquisition: B.R.A., A.K.Y. and S.S.; investigation: B.R.A., U.B.S., H.M., B.B., C.A.H., A.K.Y. and S.S; methodology: B.R.A., U.B.S. and S.S.; project administration: B.R.A. and S.S.; resources: B.R.A., C.A.H., A.K.Y. and S.S.; software: B.R.A. and U.B.S.; supervision: B.R.A., A.K.Y. and S.S.; visualization: B.R.A., U.B.S., H.M. and B.B.; writing – original draft: B.R.A., U.B.S. and S.S.; writing – review and editing: B.R.A., U.B.S., H.M., B.B., C.A.H., A.K.Y. and S.S.

Competing interests. We declare we have no competing interests.

Funding. This work was supported by the National Science Foundation under a Postdoctoral Research Fellowship in Biology DBI 1812107 to B.R.A.; a Faculty Early Career Development Award no. 1554790 to S.S.; DBI grant no. 1349345, DEB grant no. 1557007 and IOS grant no. 1920895 to A.Y.K.; and a Dunn Family Professorship to S.S.

Acknowledgements. We thank Jesse Barber, Stephanie Gage, Jeff Gau, Teá Kesting-Handly, Megan Matthews, Izaak Neveln, David Plotkin, Joy Putney, Juliette Rubin, Varun Sharma, Ryan St Laurent and Travis Tune for helpful discussions, Aaron Olsen for assistance with image digitization and analysis, Bo Cheng and Yagiz Bayiz for advice on the aerodynamic blade element model and Laurel Kaminsky for assistance in imaging museum specimens.

References

1. Nicholson DB, Ross AJ, Mayhew PJ. 2014 Fossil evidence for key innovations in the evolution of insect diversity. *Proc. R. Soc. B* **281**, 20141823. (doi:10.1098/rspb.2014.1823)
2. Warrick DR, Dial KP. 1998 Kinematic, aerodynamic and anatomical mechanisms in the slow, maneuvering flight of pigeons. *J. Exp. Biol.* **201**, 655–672. (doi:10.1242/jeb.201.5.655)
3. Sane SP. 2003 The aerodynamics of insect flight. *J. Exp. Biol.* **206**, 4191–4208. (doi:10.1242/jeb.00663)
4. Pesavento U, Wang ZJ. 2009 Flapping wing flight can save aerodynamic power compared to steady flight. *Phys. Rev. Lett.* **103**, 118102. (doi:10.1103/PhysRevLett.103.118102)
5. Orlowski CT, Girard AR. 2012 Dynamics, stability, and control analyses of flapping wing micro-air vehicles. *Prog. Aerosp. Sci.* **51**, 18–30. (doi:10.1016/j.paerosci.2012.01.001)
6. Wootton RJ. 1992 Functional-morphology of insect wings. *Annu. Rev. Entomol.* **37**, 113–140. (doi:10.1146/annurev.en.37.010192.000553)
7. Combes S, Daniel T. 2003 Flexural stiffness in insect wings I. Scaling and the influence of wing venation. *J. Exp. Biol.* **206**, 2979–2987. (doi:10.1242/jeb.00523)
8. Le Roy C, Debat V, Llaurens V. 2019 Adaptive evolution of butterfly wing shape: from morphology to behaviour. *Biol. Rev.* **94**, 1261–1281. (doi:10.1111/brv.12500)
9. Aiello BR *et al.* 2021 Adaptive shifts underlie the divergence in wing morphology in bombycoid moths. *Proc. R. Soc. B* **288**, 20210677. (doi:10.1098/rspb.2021.0677)
10. Dudley R. 1991 Biomechanics of flight in neotropical butterflies: aerodynamics and mechanical power requirements. *J. Exp. Biol.* **159**, 335–357. (doi:10.1242/jeb.159.1.335)
11. Fei YHJ, Yang JT. 2016 Importance of body rotation during the flight of a butterfly. *Phys. Rev. E* **93**, 1–10. (doi:10.1103/PhysRevE.93.033124)
12. Sane SP, Dickinson MH. 2002 The aerodynamic effects of wing rotation and a revised quasi-steady model of flapping flight. *J. Exp. Biol.* **205**, 1087–1096. (doi:10.1242/jeb.205.8.1087)
13. Han JS, Kim JK, Chang JW, Han JH. 2015 An improved quasi-steady aerodynamic model for insect wings that considers movement of the center of pressure. *Bioinspir. Biomim.* **10**, 046014. (doi:10.1088/1748-3190/10/4/046014)
14. Bomphrey RJ, Nakata T, Phillips N, Walker SM. 2017 Smart wing rotation and trailing-edge vortices enable high frequency mosquito flight. *Nature* **544**, 92–95. (doi:10.1038/nature21727)
15. Wang JK, Sun M. 2005 A computational study of the aerodynamics and forewing-hindwing interaction of a model dragonfly in forward flight. *J. Exp. Biol.* **208**, 3785–3804. (doi:10.1242/jeb.01852)
16. Kawahara AY *et al.* 2019 Phylogenomics reveals the evolutionary timing and pattern of butterflies and moths. *Proc. Natl Acad. Sci. USA* **116**, 22 657–22 663. (doi:10.1073/pnas.1907847116)
17. Hamilton CA, St Laurent RA, Dexter K, Kitching IJ, Breinholt JW, Zwick A, Timmermans M, Barber JR, Kawahara AY. 2019 Phylogenomics resolves major relationships and reveals significant diversification rate shifts in the evolution of silk moths and relatives. *BMC Evol. Biol.* **19**, 182. (doi:10.1186/s12862-019-1505-1)
18. Janzen DH. 1984 Two ways to be a tropical big moth: Santa Rosa saturniids and sphingids. In *Oxford surveys in evolutionary biology*, vol. 1 (eds R Dawkins, M Ridley), pp. 85–140. Oxford, UK: Oxford University Press.
19. Tuskes PM, Tuttle JP, Collins MM. 1996 *The wild silk moths of North America: a natural history of the Saturniidae of the United States and Canada*. Ithaca, NY: Cornell University Press.
20. Tuttle J. 2007 *The hawk moths of North America: a natural history study of the Sphingidae of the United States and Canada*. Wedge Entomological Research Foundation.
21. Wasserthal L. 1993 Swing-hovering combined with long tongue in hawkmoths, an antipredator adaptation during flower visits. In *Animal-plant interactions in tropical environments* (eds W Barthlott, CM Naumann, K Schnidt-Loske, KL Schuchmann), pp. 77–87. Annual Meeting of the German Society for Tropical Ecology. Bonn, Germany: Zoologisches Forschungsinstitut und Museum Alexander Koenig.
22. Farina WM, Varju D, Zhou Y. 1994 The regulation of distance to dummy flowers during hovering flight in the hawk moth *Macroglossum stellatarum*. *J. Comp. Physiol. A-Sensory Neural and Behav. Physiol.* **174**, 239–247. (doi:10.1007/BF00193790)
23. Sprayberry JDH, Daniel TL. 2007 Flower tracking in hawkmoths: behavior and energetics. *J. Exp. Biol.* **210**, 37–45. (doi:10.1242/jeb.02616)
24. Sponberg S, Dyhr JP, Hall RW, Daniel TL. 2015 Luminance-dependent visual processing enables moth flight in low light. *Science* **348**, 1245–1248. (doi:10.1126/science.aaa3042)
25. Stöckl AL, Kihlström K, Chandler S, Sponberg S. 2017 Comparative system identification of flower tracking performance in three hawkmoth species

reveals adaptations for dim light vision. *Phil. Trans. R. Soc. B* **372**, 20160078. (doi:10.1098/rstb.2016.0078)

26. Anderson JD. 2017 *Fundamentals of aerodynamics*, 6th edn. New York, NY: McGraw-Hill Education.
27. Ros IG, Bassman LC, Badger MA, Pierson AN, Biewener AA. 2011 Pigeons steer like helicopters and generate down- and upstroke lift during low speed turns. *Proc. Natl Acad. Sci. USA* **108**, 19 990–19 995. (doi:10.1073/pnas.1107519108)
28. Greeter JS, Hedrick TL. 2016 Direct lateral maneuvers in hawkmoths. *Biol. Open* **5**, 72–82. (doi:10.1242/bio.012922)
29. Jacobs DS, Bastian A. 2016 *Predator-prey interactions: co-evolution between bats and their prey*. Cham, Switzerland: Springer.
30. Lewis FP, Fullard JH, Morrill SB. 1993 Auditory influences on the flight behavior of moths in a Nearctic site. 2. Flight times, heights, and erraticism. *Can. J. Zool.-Revue Canadienne De Zoologie* **71**, 1562–1568. (doi:10.1139/z93-221)
31. Cheng B, Tobalske BW, Powers DR, Hedrick TL, Wang Y, Wethington SM, Chiu GTC, Deng XY. 2016 Flight mechanics and control of escape manoeuvres in hummingbirds. II. Aerodynamic force production, flight control and performance limitations. *J. Exp. Biol.* **219**, 3532–3543. (doi:10.1242/jeb.137570)
32. Ellington CP. 1984 The aerodynamics of hovering insect flight. VI. Lift and power requirements. *Phil. Trans. R. Soc. Lond. B* **305**, 145–181. (doi:10.1098/rstb.1984.0054)
33. Willmott AP, Ellington CP. 1997 The mechanics of flight in the hawkmoth *Manduca sexta*. II. Aerodynamic consequences of kinematic and morphological variation. *J. Exp. Biol.* **200**, 2723–2745. (doi:10.1242/jeb.200.21.2723)
34. Warfvinge K, KleinHeerenbrink M, Hedenstrom A. 2017 The power-speed relationship is U-shaped in two free-flying hawkmoths (*Manduca sexta*). *J. R. Soc. Interface* **14**, 20170372. (doi:10.1098/rsif.2017.0372)
35. Olsen AM, Westneat MW. 2015 StereoMorph: an R package for the collection of 3D landmarks and curves using a stereo camera set-up. *Methods Ecol. Evol.* **6**, 351–356. (doi:10.1111/2041-210X.12326)
36. Ellington CP. 1984 The aerodynamics of hovering insect flight. 2. Morphological parameters. *Phil. Trans. R. Soc. Lond. B* **305**, 17–40. (doi:10.1098/rstb.1984.0050)
37. Matthews M, Sponberg S. 2018 Hawkmoth flight in the unsteady wakes of flowers. *J. Exp. Biol.* **221**, jeb179259. (doi:10.1242/jeb.179259)
38. Knorlein BJ, Baier DB, Gatesy SM, Laurence-Chasen JD, Brainerd EL. 2016 Validation of XMALab software for marker-based XROMM. *J. Exp. Biol.* **219**, 3701–3711. (doi:10.1242/jeb.145383)
39. Kim J-K, Han J-S, Lee J-S, Han J-H. 2015 Hovering and forward flight of the hawkmoth *Manduca sexta*: trim search and 6-DOF dynamic stability characterization. *Bioinspir. Biomim.* **10**, 56012. (doi:10.1088/1748-3190/10/5/056012)
40. Dickinson MH, Lehmann F-O, Chan WP. 1998 The control of mechanical power in insect flight. *Am. Zool.* **38**, 718–728. (doi:10.1093/icb/38.4.718)
41. Gau J, Gravish N, Sponberg S. 2019 Indirect actuation reduces flight power requirements in *Manduca sexta* via elastic energy exchange. *J. R. Soc. Interface* **16**, 20190543. (doi:10.1098/rsif.2019.0543)
42. Muijres FT, Iwasaki NA, Elzinga MJ, Melis JM, Dickinson MH. 2017 Flies compensate for unilateral wing damage through modular adjustments of wing and body kinematics. *Interface Focus* **7**, 20160103. (doi:10.1098/rsfs.2016.0103)
43. Fernandez MJ, Driver ME, Hedrick TL. 2017 Asymmetry costs: effects of wing damage on hovering flight performance in the hawkmoth *Manduca sexta*. *J. Exp. Biol.* **220**, 3649–3656. (doi::10.1242/jeb.153494)
44. Norberg UM, Rayner JMV. 1987 Ecological morphology and flight in bats (Mammalia, Chiroptera): wing adaptations, flight performance, foraging strategy and echolocation. *Phil. Trans. R. Soc. Lond. B* **316**, 337–419. (doi:10.1098/rstb.1987.0030)
45. Pennycuick CJ. 1968 Power requirements for horizontal flight in pigeon *Columba livia*. *J. Exp. Biol.* **49**, 527–555. (doi:10.1242/jeb.49.3.527)
46. Aiello BR, Westneat MW, Hale ME. 2017 Mechanosensation is evolutionarily tuned to locomotor mechanics. *Proc. Natl Acad. Sci. USA* **14**, 4459–4464. (doi:10.1073/pnas.1616839114)
47. Warrick DR, Dial KP, Biewener AA. 1998 Asymmetrical force production in the slow maneuvering flight of pigeons. *Auk* **115**, 916–928. (doi:10.2307/4089510)
48. Hedrick TL, Cheng B, Deng X. 2009 Wingbeat time and the scaling of passive rotational damping in flapping flight. *Science* **324**, 252–255. (doi:10.1126/science.1168431)
49. Fry SN, Sayaman R, Dickinson MH. 2005 The aerodynamics of hovering flight in *Drosophila*. *J. Exp. Biol.* **208**, 2303–2318. (doi:10.1242/jeb.01612)
50. Dickinson MH, Muijres FT. 2016 The aerodynamics and control of free flight manoeuvres in *Drosophila*. *Phil. Trans. R. Soc. B* **371**, 20150388. (doi:10.1098/rstb.2015.0388)
51. Dudley R, Ellington C. 1990 Mechanics of forward flight in bumblebees: II. Quasi-steady lift and power requirements. *J. Exp. Biol.* **148**, 53–88. (doi:10.1242/jeb.148.1.53)
52. Dudley R, Ellington C. 1990 Mechanics of forward flight in bumblebees: I. Kinematics and morphology. *J. Exp. Biol.* **148**, 19–52. (doi:10.1242/jeb.148.1.19)
53. Jourjine N, Hoekstra HE. 2021 Expanding evolutionary neuroscience: insights from comparing variation in behavior. *Neuron* **109**, 1084–1099.
54. Aiello B. 2021 Data from: The evolution of two distinct strategies of moth flight. Dryad Digital Repository. (doi:10.5061/dryad.3ffbg79jp)